Magnetic properties of a cobalt(II) dimer of pseudo tetrahedral geometry $[Co_2\{(CO)_9Co_3C–COO\}_5, C_{14}H_{19}N_2H]$

Victor Calvo-Perez *, Evgenia Spodine

Facultad Ciencias Químicas y Farmacéuticas, Centro para la Investigación Interdisciplinaria Avanzada en Ciencia de los Materiales, Universidad de Chile, Casilla 233, Santiago, Chile

Abstract

The crystalline ion pair $[Co_2\{OOC–CCo_3(CO)_9\}_5, C_{10}H_6(N(CH_3)_2)_2H]$ (1) presents unusual magnetic properties. The X-band EPR spectrum of 1 at room temperature presents two unresolved bands at $g = 1.98$ and 4.55. At a low temperature (20 K), the cluster of clusters 1 presents a complicated spectrum with an intense signal at 1700 G. The magnetic susceptibility of 1 was fit to a two spin $S_1 = S_2 = 3/2$ Heisenberg model, with $J = 11.2$ cm^{-1} and a g value of 2.3. There is no field dependence of the magnetization, which suggests *intramolecular coupling* between the two tetrahedral centers of the cluster. Molecular orbital modeling indicates a sigma path of exchange between two topologically non-equivalent cobalt(II) centers.

Keywords: Magnetic properties; Cobalt(II) dimers; Magnetic susceptibility; Molecular orbital modeling; Cluster of clusters

1. Introduction

The magnetic properties of Co(II) with the pseudo-tetrahedral environment have been rationalized mainly for cobalt–halides [1] and pyrazolate bridged dicobalt-complexes [2]. There is only one example of mononuclear Co(II) carboxylates [3] with tetrahedral geometry and a magnetic moment of 4.55/BM; most of the Co(II) carboxylate structures present higher coordination numbers. Catterick et al. report an interesting case of mixed tetrahedral and octahedral Co(II) sites for their $[Co_3(benzoate)_6(quinoline)_2]$ [4], where two pseudo-tetrahedral cobalt centers are separated by 2.56 Å from a central cobalt atom in octahedral geometry. The Co(II) atoms in this compound are only slightly antiferromagnetically coupled down to 98 K. More recently $[Co_3(OCOCH_3)_8]^{2-}$ has been reported to have Co(II) centers in a distorted octahedral environment. The magnetic measurements indicate antiferromagnetic coupling, with a $\mu_{eff} = 4.39$ BM, at 4 K [5]. Besides, a well-known cobalt(II) tetramer with a μ_4-oxo center has been described, $Co_4O(pivalate)_6$, and magnetically characterized. The core of four pseudo-tetrahedral Co(II) is surrounded by six pivalate ligands. The oxo bridge together with the carboxylate bridges transmit a weak antiferromagnetic coupling, with a μ_{eff} being 3.86 BM per cobalt atom at 296 K.

On the other hand, the oxidation of the organometallic cluster $(CO)_9Co_3C–COOH$ (FaH) occurs with the formation of Co(II) and the subsequent assembly of the $Co_4O(Fa)_6$ cluster of clusters [6]. This cluster of clusters resembles structurally [7], as well as magnetically, the $Co_4O(pivalate)_6$ complex. $Co_4O(Fa)_6$ was reported to show a broad EPR signal at $g = 4.00$ in CH_3CN glass at 10 K, indicative of the presence of cobalt(II). The four tetrahedral Co(II) in the core of $Co_4O(Fa)_6$ system are antiferromagnetically coupled with $\mu_{eff} = 4.75$ BM and θ: -27 K.

Starting from the same cluster, (FaH) and bis-(dimethylamino)-naphthalene, we obtained a cluster of clusters with two pseudo-tetrahedral Co(II) centers bridged by three carboxylate groups, $[Co_2\{OOC–CCo_3(CO)_9\}_5, C_{10}H_6(N(CH_3)_2)_2H]\ C_6H_5CH_3$ (1) [9]. This cluster of clusters presents three bridging carboxylate ligands with two pseudo-tetrahedral Co(II) separated enough to have a non-bonding

* Corresponding author.

situation (3.45 Å). Shorter Co(II)–Co(II) distances of 2.265 Å are better described as single bonds, and the dimers with such interatomic distances are diamagnetic [10].

The aim of this work was to magnetically characterize the cluster of clusters **1**, and its properties will be reported here in relation to the structural characteristics and MO analysis. Magnetic exchange interactions are known to occur through carboxylate bridges in many metallic systems such as copper(II) [11] where a σ exchange path is postulated to carry the magnetic interaction. However, no theoretical work has been done on tetrahedral cobalt carboxylates, nor in open shell dimeric systems like that in cluster of clusters **1**.

2. Experimental

2.1. Materials

Proton sponge $C_{10}H_6(N(CH_3)_2)_2$ (Ps) was purchased from Aldrich and sublimed under vacuum (10 mTorr) at 30°C on a Schlenk line. All the solvents used were distilled under nitrogen just before the preparation. All reactions were performed under argon on a Schlenk line using standard air free methods.

The cluster tricobalt-nonacarbonyl methylidene carboxylic acid, $(CO)_9Co_3C$–COOH (FaH) was prepared from $Co_2(CO)_8$ purchased from Strem, and reacted with Cl_3C–$COOCH(CH_3)_2$ in toluene according to Seyfert's method [12].

2.2. Preparation of cluster of clusters 1

The cluster of cluster was prepared as reported previously [9] and recrystallized from warm CH_2Cl_2 under Ar. The solution in methylene chloride was layered with freshly distilled toluene, and the product was identified by IR spectroscopy.

2.3. Physical measurements

IR spectra were recorded on a Brucker FT-IR spectrometer IFS 28 as KBr pellets. EPR spectra ware recorded on a Brucker 1600 spectrometer, working on the X-band (9.36 GHz), and equipped with an Oxford variable temperature controller. In a typical experiment 5 mg of a crystalline sample of **1** where placed in a quartz capillary tube sealed under vacuum. Microwave power was set at 100 mW, while modulation amplitude was kept low (5 G). The amplifier gain was 10 000 and the signal averaged five times to improve the signal to noise ratio. EPR spectra of CH_2Cl_2 solutions were obtained in a 2 mm quartz capillary under argon.

Magnetic susceptibility: 63.66 mg of crystalline $C_{69}H_{19}N_2Co_{17}O_{55}$ (**1**), were placed in a gelatin capsule and χ measured with a SQUID-SHE magnetometer. The applied magnetic field was set at 0.1 T. Experimental data were corrected for diamagnetic contributions for the counterion (PsH) and cluster groups (988×10^{-6} cm^3 mol^{-1}).

3. Results and discussion

3.1. IR spectra

The CO stretching of the metal carbonyl as well as the carboxylate groups dominates the vibrational spectrum of the cluster of clusters **1**. The strongest band corresponds to the group vibrations of metal carbonyls at 2068 cm^{-1}. The second most important feature of the cluster of clusters is the double peak observed in the region between 1370 and 1390 cm^{-1} corresponding to the symmetric stretching vibration of the carboxylates. This region of the vibrational spectrum shows clearly a RCOO bridging situation. The medium peak observed for **1** at 1542 cm^{-1} is the antisymmetric stretch of the carboxylate. The observed $\Delta\nu_{COO}$ 159 cm^{-1} indicates a bridging carboxylate. IR of compound **1** shows at least two different kinds of COO stretching; the medium band at 1542 cm^{-1} is probably arising from the bridging carboxylates, while the broad and weak band at 1579 cm^{-1} corresponds to the terminal carboxylates. The structure of cluster **1** is presented in Fig. 1, notice that one axial Fa is chelating and in the neighboring Co(II) the Fa ligand is monodentate (Table 1).

Comparing the IR spectrum of FaH and Co_4OFa_6 with that of compound **1**, it is possible to conclude that the COO stretching patterns are a good indicator of the coordination mode of these groups. In addition, the close resemblance of the CO stretching region in these three different clusters indicates that the $(CO)_9Co_3C$– groups are not involved greatly in charge delocalization of the Co(II) centers in the ground state, as compared to other clusters of clusters such as Cr(II), Mo(II) and W(II) where backdonation shifts the CO stretching band as much as 10 cm^{-1} [13]. Therefore, this information allows us to postulate that magnetic properties are restricted to the Co(II) carboxylate manifold.

3.2. EPR spectra

The X-band EPR spectrum of the cluster of clusters **1** is observed at room temperature (r.t.) as two unresolved bands (Fig. 2). The spectrum of **1** is of an axial pattern with a strong resonance at g: 1.98, along with a weaker resonance at g: 4.55. The first signal can be interpreted as originating from the lower Kramers doublet, while the second from the upper Kramers doublet [14]. The EPR spectrum of Co_4OFa_6 has been reported to be a broad featureless band in CH_3CN solution at 10

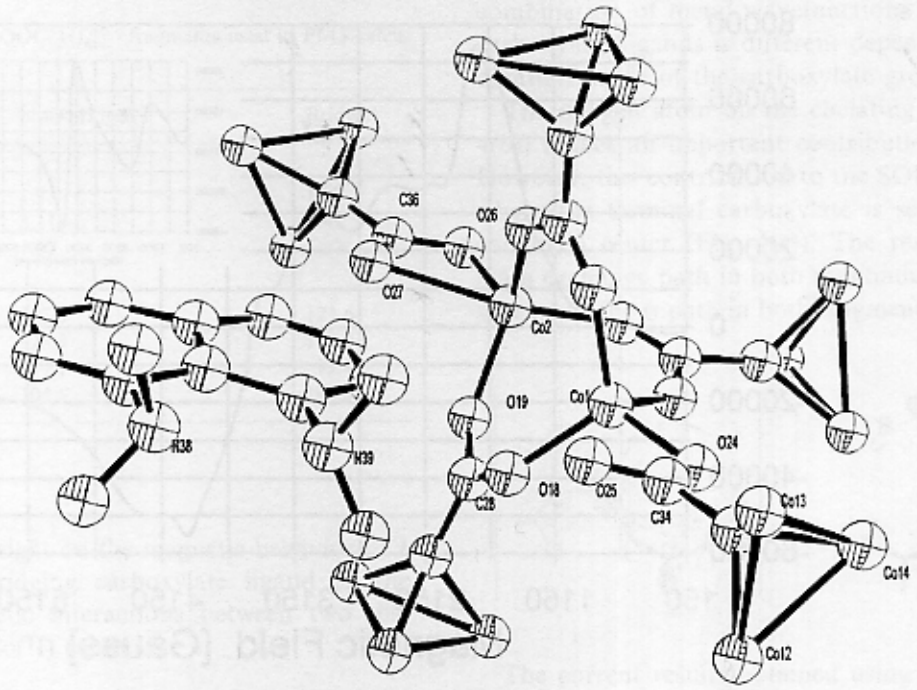

Fig. 1. Structure of $[Co_2\{(CO)_9Co_3C\text{–}COO\}_5]$ anion viewed along a pseudo C3 axis. CO groups omitted for clarity, proton sponge counterion shown to the left (from Ref. [9]).

K, occurring at $g = 4.0$ [8], as is observed in the spectrum of cluster **1**. The spin–spin coupling between two or more Co(II) centers precludes the observation of the hyperfine structure in this multinuclear compound (usually ~ 50 G for monomeric Co(II) centers).

Cluster of clusters **1** shows a complicated spectrum as the temperature drops to 20 K, with an intense signal around 1700 G (Fig. 2). Other transition metals, such as Mn(II) coupled with organic radicals, are also reported to present a temperature sensitive spectrum [15]. This fact implies that a magnetic coupling dominates at low temperatures in the cluster of clusters **1**.

3.3. Magnetic susceptibility of cluster of clusters 1

The temperature dependence of the magnetic moment for the crystalline sample of the cluster of clusters **1** is shown Fig. 3. (μ_{eff} varies from 4.6 BM at 298 K to 5.4 BM at 5 K). The magnetic moment calculated near room temperature for the crystals has a similar value to that obtained by Evans method in solution ($\mu_{eff} = 4.08$ BM). These results together with the IR spectrum of **1** in CH_2Cl_2 solution permit us to postulate the integrity of the cluster in solution.

The spin Hamiltonian used for two interacting cobalt (II) centers was

$$H = -2J\bar{S}_1\bar{S}_2$$

The experimental data were fitted by an equation for two 3/2 interacting spins ($S_1 = S_2 = 3/2$) corrected for paramagnetic impurities, ρ, and temperature independent paramagnetism, TIP [16].

$$\chi_{cor} = (1-p)\cdot\chi_H + p\cdot\chi_P + \mathrm{TIP}$$

$$\chi_H = C\frac{2e^{2x} + 10e^{6x} + 28e^{12x}}{1 + 3e^{2x} + 5e^{6x} + 7e^{12x}}$$

$$x = -J/kT$$

$$C = Ng^2\beta^2/kT$$

where J expresses the intramolecular exchange interaction, $\bar{S}_1$ and $\bar{S}_2$ are quantum spin operators and N, β, g and T have their usual meaning. Three sets of data were fitted using constant values of 0.0068 (TIP) and 2.33 (g). The paramagnetic impurity was assumed to have a Curie behavior. A non-linear least-square fit of 42 observed data leads to the value of $J = 11.2$ cm^{-1} and

Table 1
Spectroscopic data for FaH, cluster of cluster $Co_2Fa_5^-$ (1) and Co_4OFa_6

	FaH	Co_2Fa_5 (1)	Co_4OFa_6
CO stretch	2111(w)	2110(m)	2109(w)
CO stretch	2051(s)	2068(s)	
CO stretch	2034(s)	2040(s)	2042(s)
COO stretch		1579(w)	
COO stretch Antisymmetric	1642(m)	1542(m)	1538(m)
COO stretch Symmetric	1380(m)	1383(m)	1383(m)

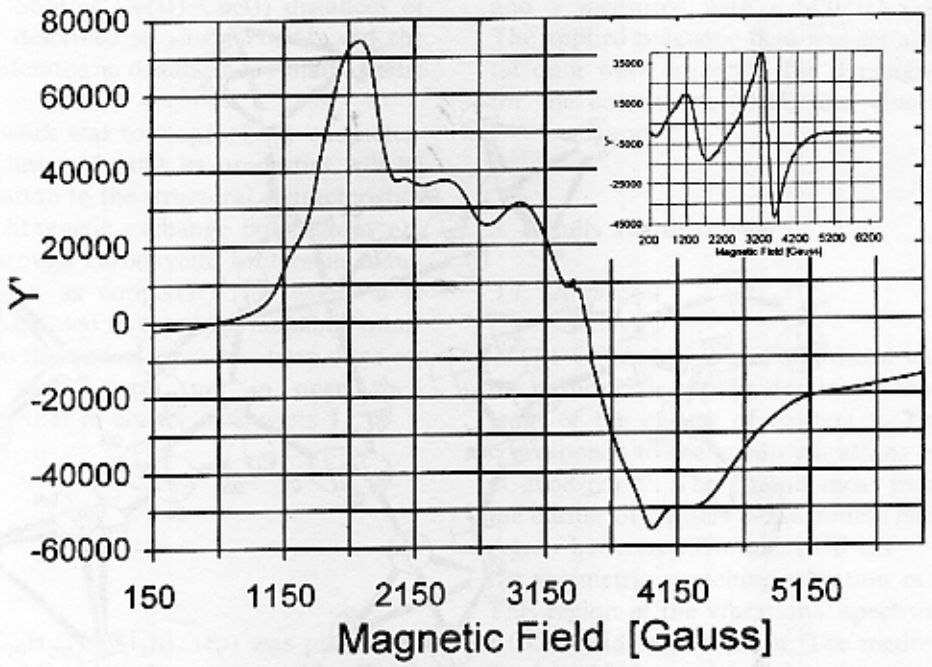

Fig. 2. EPR spectrum of crystals of 1 at 20 K under vacuum. Insert: EPR spectrum of crystals of 1 at 293 K.

$R = 1.3 \times 10^{-3}$ for **1**. This positive J value is characteristic of a weak ferromagnetic interaction between the local quadruplets. The increase in magnetic moment together with observed enhanced intensity of the EPR spectrum as the temperature is lowered from 293 to 20 K can be considered due to the ferromagnetic nature of the intradimer interaction which dominates below 20 K [1] (Fig. 2).

Magnetization measurements were performed as a function of magnetic field, but no bulk cooperativity was observed. However a small magnetization remained after the field was turned off at 2.4 K.

The different sign of the weak intramolecular coupling in **1** from that in the pyrazolate bridged cobalt(II) dimer [2], which has antiferromagnetic behavior, can be understood on the basis of the different bridging mode of both compounds. As seen in the scheme below the exchange magnetic pathway is defined by O–C–O set of atoms for **1** and N–N set of atoms for the pyrazolate bridged dimer.

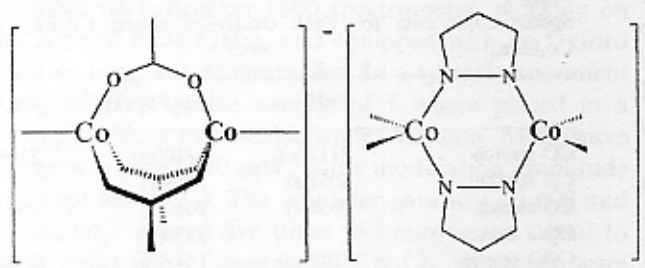

This structural feature is important as far as magnetic coupling is concerned, since according to a recent magneto-structural study, the electronegativity of the donor atoms affects the delocalization of the spin on the bridge [17]. Besides the topology, differences occurring between the two Co(II) atoms in **1** (face sharing), as compared to the pyrazolate bridged dimer (edge sharing), may be the key to the orthogonality of the orbitals involved in **1** [18].

The sign of the magnetic coupling in **1** is opposite to that reported for the carboxylate bridged Co(II) linear trimer [5], where the coupling between adjacent Co(II) centers of pseudo-octahedral geometry is antiferromagnetic in nature ($J = -7.0$ cm^{-1}). This could be the consequence of the fact that the unpaired electrons on each Co(II) center in these compounds are described by different magnetic orbitals in each case.

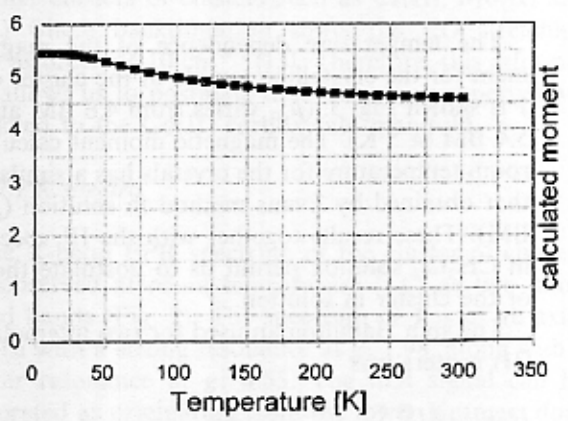

Fig. 3. Magnetic moment of a crystalline sample of **1** measured at 0.1 T, --- calculated moment according to $S_1 = S_2 = 3/2$ Heisenberg model.

Table 2
Structural details of $[Co(OOC–H)_4]^{2-}$ fragments used in PM3 calculations

	Non-bridged	Bridged
Distances (Å)		
O′–Co	1.93	1.97
O″–Co	3.11	2.41
O–Co	1.97	1.97
Angles (°)		
O–C–O	125.6	125.6
O′–C–O″	123.8	110.0
Co–O′–C	117.1	99.4
O–Co–O	104.5	105.4

To get a better insight on the magnetic behavior of **1** we modeled the bridging carboxylate ligand as the pathway for magnetic interactions between two distorted tetrahedral Co(II) centers.

3.4. Molecular modeling the cluster of clusters 1

The aim of these calculations was to find a plausible way for the magnetic exchange between two different cobalt(II) centers and to display the actual magnetic orbitals. In a first attempt each cobalt fragment surrounded by its four carboxylate ligands was modeled. In the second place, the carboxylate manifold for the cobalt(II) dimer was studied just as found in the cluster of clusters **1**. As described above, the metal carbonyls are not involved in charge delocalization, therefore the $(CO)_9Co_3C$ groups were excluded from these calculations, i.e. an isolated $[Co_2(OOC–H)_5]^-$ group with bond distances and angles taken from the actual structure are used in these calculations. Besides, these calculations have to account for the spin multiplicity of the metal centers, therefore these carboxylate manifolds were explored by using the semi-empirical method SPARTAN PM3 [19,20].

Distortions from the tetrahedral geometry were also studied for the ^4A state of the two isolated $[Co(OOC–H)_4]^{2-}$ fragments as found in the actual structure of **1** (see Table 2).

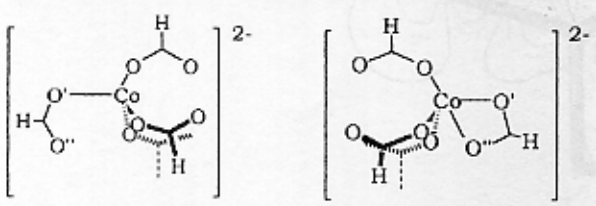

The bridging carboxylates are essentially planar, therefore the interactions between the 3d orbitals and the carboxylate σ and π system were investigated. The combination of metal wavefunctions with those of the carboxylate ligands is different depending on the coordination mode of the carboxylate group.

The oxygen atom on the chelating carboxylate (Fig. 4(b)) makes an important contribution to the SOMO. However, this contribution to the SOMO is not present where the terminal carboxylate is separated from the cobalt(II) center (Fig. 4(a)). The results indicate one main exchange path in both mononuclear fragments. A scheme of the σ path in both fragments is shown below.

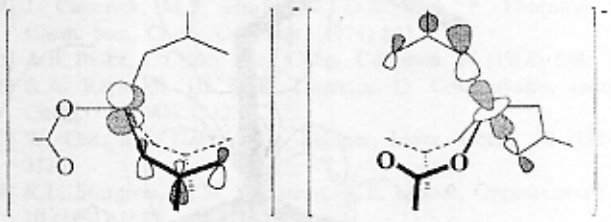

The current results obtained using the PM3 method (including quartet spin state for both mononuclear cobalt(II) centers) indicate that chelation introduces an important perturbation to the metal orbitals.

The efforts to model the $[Co_2(OOCR)_5]^-$ system were only successful with a semi-empirical method (PM3) that accounts for the spin multiplicity expected from the current magnetic measurements. This method has been used successfully in the study of magnetic interaction between two copper(II) centers [19] and a variety of organometallic compounds [20] with a great success in the prediction of the actual geometries [21].

For the sake of simplicity, the quintuplet of the idealized core of the cluster of clusters was studied, i.e. $[Co_2(OOC–H)_5]^-$. The structural details were taken from the actual structure of the cluster of clusters **1** and summarized in Table 2. The calculations show that the SOMO and the nearby filled molecular orbitals are composed of Co 3d functions as well as a σ system of the bridging carboxylates as shown below.

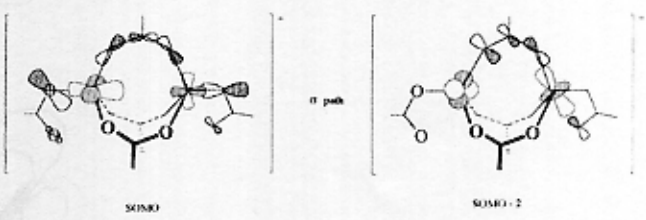

A slice of the SOMO shows two different 3d orbitals together with the bridging carboxylate (see Fig. 4(c)). Interestingly the two cobalt(II) 3d orbitals involved in the SOMO are accidentally orthogonal due to the unex-

pected participation of the chelating carboxylate. This occurs not only in the SOMO but also in the MOs underneath the SOMO. In the scheme above, it is shown that both SOMO and SOMO-2 present an important participation of the chelating carboxylate in the σ path. The chelating carboxylate not only adds a fraction of p character to the MO but also combines with the symmetry appropriate metal orbitals (d_{z^2} or $d_{x^2-y^2}$, respectively). This combination of the metal orbitals with the chelating oxygen orbitals makes the two cobalt(II) centers non-equivalent. Besides, the chelating carboxylate combines with cobalt(II) on a σ path but not with the neighbor cobalt(II), hence making this σ path suitable for a ferromagnetic exchange

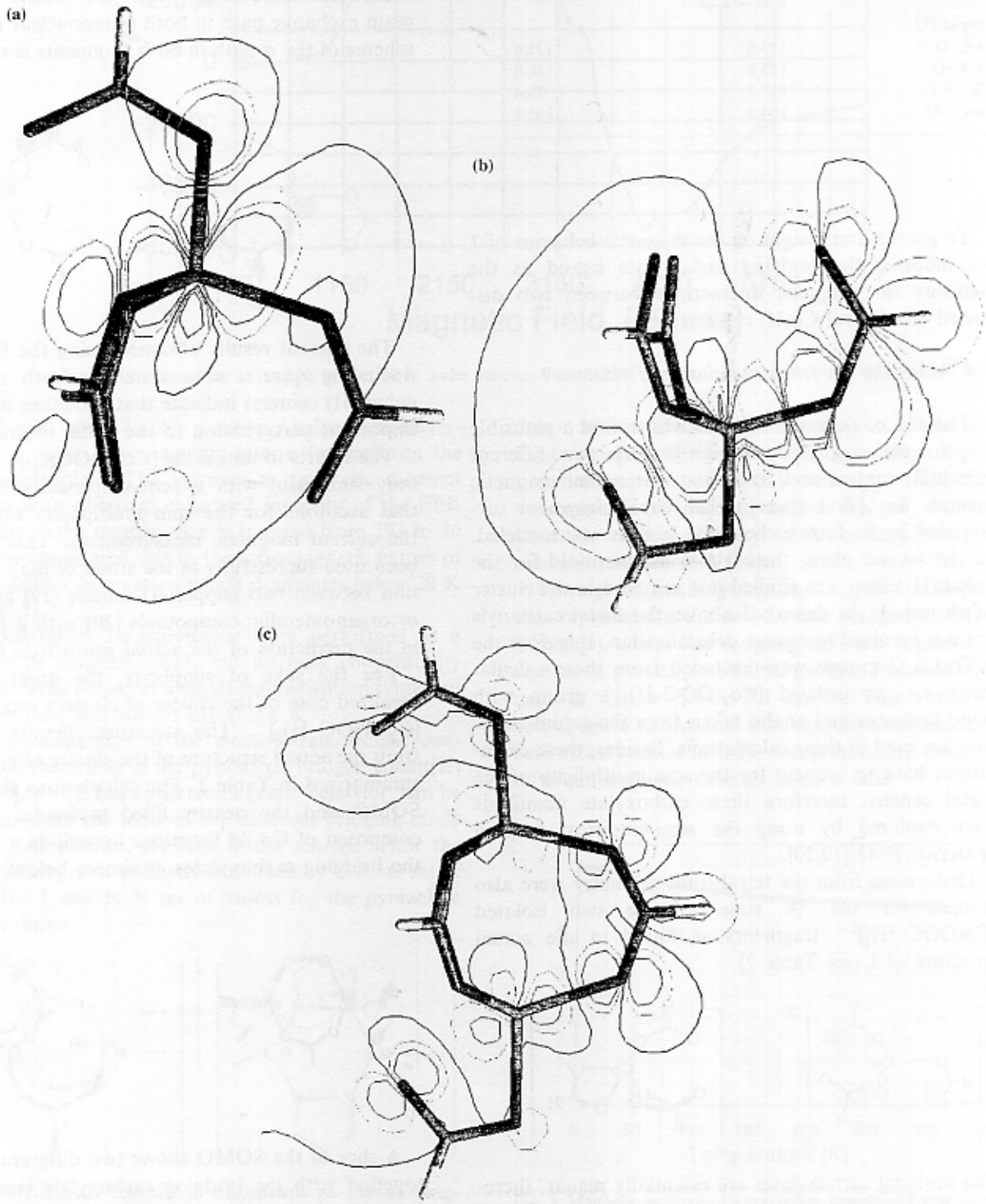

Fig. 4. (a) Slice of the SOMO of the $[Co(OOC–H)_4]^{2-}$ fragment. (b) Slice of the SOMO of the chelate $[Co(OOC–H)_4]^{2-}$ fragment. (c) Slice of the SOMO-2 of the model compound $[Co_2(OOC–H)_5]^-$.

[22]. The alternative π path also occurs in this system (not shown), though it is frequently less important in transmitting a magnetic interaction because of the smaller overlap between the adjacent p functions of the carboxylate group.

In view of the MO analysis, we postulate the presence of the bridging carboxylate on one cobalt(II) center as the origin of the non-equivalence, and therefore the observed ferromagnetic coupling in **1** occurs through the σ path on the bridging carboxylate.

4. Concluding remarks

Cluster **1** presents an interesting case of two interacting paramagnetic centers linked via carboxylates. The magnetic characteristics of **1** are due to the intramolecular coupling between two pseudo tetrahedral Co(II) centers. The nearest distance between two Co(II) dimers is about 10 Å, making it impossible to observe any further intermolecular magnetic coupling. Related tetrahedral Co(II) carboxylates $Co_4O(RCOO)_6$ (where R = pivalate, Fa) have been reported briefly but the origin of the EPR and magnetic susceptibility have not been discussed in relation to its structure, aiming at the complexity of the exchange paths. A complete analysis of the correlation and exchange energy (Dft methods) between two or more Co(II) centers is not possible at the moment because the magnitude of the spin–orbit coupling ($-147\ cm^{-1}$) is larger than the observed spin–spin coupling. Further analysis of the magnetic exchange path is underway using semi-empirical methods, because it provides a useful qualitative explanation of the origin of the magnetic phenomena in Co(II) centers.

Acknowledgements

The support from the DID Universidad de Chile, Fondo Nacional de Ciencias y Tecnologia (FONDECYT 198-0896) and Third World Academy of Sciences (RGA-96-472) is greatly acknowledged. We are also very grateful to Dr Octavio Peña (Universite de Rennes I, France) for the magnetic susceptibility measurements.

References

[1] R.P. VanStapele, H.G. Beljers, P.F. Bongers, H. Zijlstra, J. Chem. Phys. 44 (1966) 3719.
[2] M.K. Ehlert, S.J. Rettig, A. Storr, R.C. Thompson, J. Trotter, Can. J. Chem. 71 (1993) 1425.
[3] J.G. Bergman, F.A. Cotton, Inorg. Chem. 5 (1966) 1420.
[4] J. Catterick, M.B. Hurthouse, D.B. New, P. Thornton, J. Chem. Soc., Chem. Commun. (1974) 843.
[5] A.B. Blake, J. Chem. Soc., Chem. Commun. 16 (1966) 569.
[6] R.A. Reynolds, III, W.R. Dunham, D. Coucouvanis, Inorg. Chem. 37 (1988) 1232.
[7] W. Cen, K.J. Haller, T.P. Fehlner, Inorg. Chem. 30 (1991) 3120.
[8] R.L. Sturgeon, M.M. Olmstead, N.E. Schore, Organometallics 10 (1991) 1649.
[9] V.F. Calvo-Perez, G.P.A. Yap, A.L. Rheingold, T.P. Fehlner, Polyhedron 13 (1999) 1869.
[10] F.A. Cotton, R. Poli, Inorg. Chem. 26 (1987) 3652.
[11] S. Alvarez, M. Julve, M. Verdaguer, Inorg. Chem. 29 (1990) 4500.
[12] D. Seyferth, Adv. Organomet. Chem. 14 (1976) 97.
[13] V.F. Calvo-Perez, T.P. Fehlner, A.L. Rheingold, Inorg. Chem. 35 (1996) 7289.
[14] F.E. Mabbs, D. Collison, Electron Paramagnetic Resonance of d Transition Metal Compounds, Elsevier, Amsterdam, 1992.
[15] C. Benelli, D. Gatteschi, C. Zanchini, R.J. Doedens, M.H. Dickman, L.C. Porter, Inorg. Chem. 25 (1986) 3453.
[16] C.J. O'Connor, Prog. Inorg. Chem. 29 (1982) 203.
[17] P. Roman, C. Guzman-Miralles, A. Luque, J.I. Beitia, J. Cano, F. Lloret, M. Julve, S. Alvarez, Inorg. Chem. 35 (1996) 3741.
[18] J.B. Goodenough, Magnetism and the Chemical Bond, Robert E. Krieger, Huntington, NY, 1976.
[19] C.A. White, G.P.A. Yap, Inorg. Chem. 38 (1999) 2548.
[20] B.J. Deppmeier, A.J. Driessen, W.J. Herhe, T. Herhe, P.E. Klunzinger, L. Lou, J. Yu, SPARTAN PLUS, 1999.
[21] T. Cundari, J. Deng, J. Chem. Inform. Comp. Sci. 39 (1999) 376.
[22] O. Kahn, Angew. Chem., Intl. Ed. Engl. 24 (1985) 834.